Investigation of nuclear structure near doubly magic ^{132}Sn

Sangeeta Das[1,*] and *Arkabrata* Gupta[2]

[1]Department of Physics, Indian Institute of Engineering Science and Technology, Shibpur, Botanic Garden, Howrah 711103.

[2]Department of Basic Science and Humanities, Institute of Engineering and Management, University of Engineering and Management, Kolkata 700160.

Abstract. Large-basis shell-model calculations have been performed to investigate the excited states of ^{131,132}Sn using a newly formulated cross-shell interaction. Recent expansions of the level schemes has provided valuable structural insights. A detailed comparison of excitation energies and electromagnetic transition rates between experimental data and theoretical predictions offers a deep understanding of these nuclei. While certain transitions align well with experimental data, others show discrepancies. This observed discrepancies in some cases points the scope of improvement of theoretical results, such as fine tuning certain $\nu - \nu$ *tbme*s.

1 Introduction

The Tin isotopes with the magic proton number $Z = 50$ have been extensively studied, spanning more than a full shell closure, including the doubly magic $^{100}_{50}\mathrm{Sn}_{50}$ and $^{132}_{50}\mathrm{Sn}_{82}$. Limited information is available for ^{100}Sn — with only its mass, half-life, and some β-decay properties known [1, 2], whereas ^{132}Sn is comparatively well-studied [3, 4] . Its first excited state above 4 MeV highlights its robust shell closure, making it a benchmark for nuclear structure studies [5].

Investigating the nuclear structure around this nucleus enhances our understanding of the evolution of single-particle states in neutron-rich nuclei, particularly near shell closures [6–8]. While recent studies have significantly advanced our understanding of single-particle states in neighboring isotopes [7–9], the collective properties of ^{132}Sn remain relatively unexplored. In particular, there is a dearth of information on its low-lying excitations [10], with only a few recent experiments [11, 12] providing insights into this area. The collective behavior of nucleons, which leads to fundamental vibrational modes with quadrupole and octupole character, are sensitive parameter for shell-model calculation. These properties are crucial for constraining the extrapolation of theoretical models to neutron-rich nuclei. The nuclei near $Z = 50$, $N = 82$, can be treated well within the shell-model. However, the predictions for the doubly magic ^{132}Sn and its excited states, and corresponding electromagnetic properties have been challenging due to the large valence space encompassing both proton and neutron shells. Consequently, a very few theoretical investigation [13, 14] are available compared to experimental ones. Additionally, the theoretical calculations have been limited mainly to the

*e-mail: dsngeta@gmail.com

two low-lying excited states (2^+ and 3^-), and further exploration is needed to investigate the excited states above 5 MeV.

Most of the excited states of ^{132}Sn arise from particle-hole (p-h) configurations, where either a proton or neutron is excited across the closed shell. Coupling single-particle and single-hole states forms multiplets of excited states with minimal admixture from other configurations. The particle-hole residual interaction causes energy splitting within a multiplet. Identifying these multiplets provides insights into nuclear two-body matrix elements, which is one of the key parameter of shell-model. Additionally, experimentally measured transition rates within and between multiplets offer valuable information on the underlying single-particle structure.

In a study of J. Benito *et al.*[11], the level scheme of ^{132}Sn has been expanded by including newly observed excited state and 68 decaying γ-transition. A tentative spin-parity and also configurations of the excited levels were proposed based on experimental findings and systematic analysis of particle-hole configurations. In another work, their investigation of ^{131}Sn, described as a single neutron-hole state, refined its level scheme [15]. Lifetimes of several excited levels were measured for the first time. Prior to this work, the available information on the lifetimes of excited levels in ^{131}Sn was limited[16, 17].

In this current work, the theoretical investigation has been done to explore mainly core excited states of ^{131,132}Sn in comparison to known, newly available experimental levels and transition rates. In our recent study, we already have performed large-scale shell-model calculations to interpret the excitation energies of ^{132}Sn and its neighboring nuclei, utilizing a new cross-shell interaction [19]. Further, we aim to evaluate whether this interaction is effective enough in reproducing other experimental data related to both yrast and non-yrast states.

2 Formalism: Details of Model space and Effective interaction

The shell-model calculation has been performed using a newly formulated cross-shell interaction sm56fph [19], which has been mainly derived from two commonly used interaction-*sn*100*pn* and *CWG* interactions [20]. Both the *sn*100*pn* and *CWG* interactions are derived from the G-matrix, based on the CD-Bonn potential. The *sn*100*pn* interaction provides good predictions for spectroscopic properties of nuclei around ^{132}Sn but has limitations in describing high lying excited states, which involves cross-shell excitation. Additionally, the model spaces of these interactions are not suitable for exploring the nuclear structure of ^{132}Sn. To address these issues, this interaction has been constructed.

The neutron model space of this interaction is extended to include five orbits below the N=82 shell ($1g_{7/2}$, $2d_{5/2}$, $2d_{3/2}$, $3s_{1/2}$, $1h_{11/2}$) and three orbits above the N=82 shell ($1h_{9/2}$, $2f_{7/2}$, $3p_{3/2}$). Since the focus is on exploring the nuclear structure of nuclei ($Z \leq 54$) around ^{132}Sn, the proton model space is truncated, retaining only $\pi 1g_{7/2}$ and $\pi 2d_{5/2}$ above Z=50 to mitigate dimensionality issues. ^{100}Sn is treated as the core of the model space.

The neutron single-particle energies (below N=82 shell) of $\nu 1g_{7/2}$, $\nu 2d_{5/2}$, $\nu 2d_{3/2}$, $\nu 3s_{1/2}$, $\nu 1h_{11/2}$ are taken as -9.74, -8.97, -7.31, -7.62, -7.38 MeV as evaluated in Ref. [20] to reproduce the experimental levels of ^{131}Sn. The single-particle energies (*spe*s) of $\nu 1h_{9/2}$, $\nu 2f_{7/2}$, $\nu 3p_{3/2}$ orbits, are evaluated as 11.06, 5.718, 8.287 MeV following the experimental binding energy of ^{133}Sn with respect to (w.r.t) ^{132}Sn and its experimental excited $3/2^-_1$ and $9/2^-_1$ states. The proton single-particle energies are 0.8072 and 1.5623 MeV for $\pi 1g_{7/2}$ and $\pi 2d_{5/2}$ orbits, respectively, same as those in *sn*100*pn* interaction [20]. The details of the two body matrix elements (*tbme*) can be found in Ref. [19]. The shell-model calculations are performed using the NUSHELLX@MSU [21] and OXBASH [22] codes.

3 Results and interpretation

3.1 Results on $^{132}_{50}Sn_{82}$

In the Ref. [19], we have calculated the excitation spectra of ^{132}Sn using three different restrictions, such as 1p1h, 2p2h and 3p3h. In this present work, we shall restrict ourselves to 3p3h calculation only. Our result shows very good agreement for the yrast I^{π}= 2^+, 4^+, 5^+, 6^+, 7^+, 8^+ and 9^+ states lying in the energy range ≈ 4-5 MeV. These states primarily arise from nearly pure multiplet structures, as the excitations involve a limited number of particle and hole states, leading to minimal configuration mixing and a strong match with experimental observations. Following the work of P. Bhattacharyya *et al.* [23], these states are mainly generated from $\nu 1h^{-1}_{11/2}2f_{7/2}$ multiplet structure. In recent work, Benito *et al.* [11], also predicted the same structure for the yrast 3^+ (E_{exp}= 4.965 MeV) state. Theoretical calculations using the 3p3h excitation mode with the sm56fph interactions show strong agreement with experimental data at least for positive yrast states as shown in Fig 1. The transition probabilities for most of the yrast states have already been evaluated taking appropriate model operators, effective charges, and effective gyromagnetic factors in restricted model space as described in Ref. [19]. New experimental data on transition probabilities of some yrast as well as non-yrast states has recently become available, which we have calculated using this new interaction tabulated in table 1 .

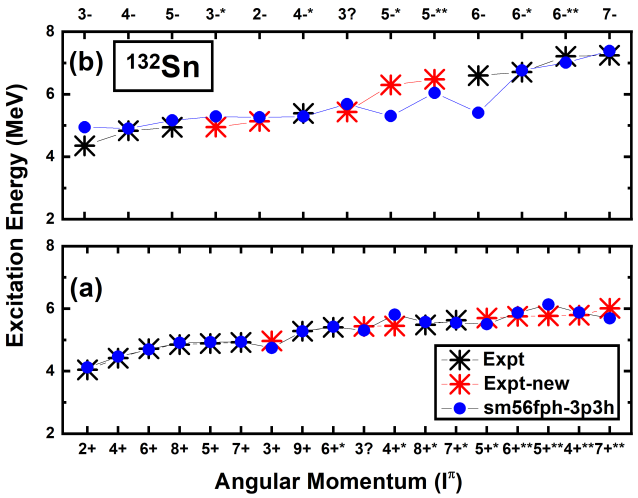

Figure 1. Comparison of theoretical prediction and experimental results for (a) positive parity and (b) negative parity states of ^{132}Sn. The experimental data from NNDC Ref. [5] and data from Ref. [11] (marked as Expt-new) are shown. The number of asterisks (n) appearing as superscript in the value of angular momentum indicates it as the (n+1)th state of that spin (X-axis).

The magnetic transition probabilities have been calculated with intrinsic proton and neutron g-factors (g^s_p and g^s_n) quenched by 0.7. In case of, electric transition probabilities neutron effective charge is taken as 1.2e to account for the limited inclusion of cross-shell neutron excitations, compensating for truncation in the model space [19].

The available data, primarily of γ-ray intensities and lifetimes, suggests dominant M1 transitions as mentioned in Ref. [11]. Assuming a pure multipole character, the transition

J_i^π	$E_i(MeV)$		J_f^π	$E_f(MeV)$		Xλ	B(Xλ)	
	Expt.	Theo.		Expt.	Theo.		Expt.	SM
5_1^+	4.886	4.929	4_1^+	4.417	4.465	M1	> 11.60	61.56
						E2	> 759	47.13
			6_1^+	4.715	4.693	M1	> 8.24	72.03
						E2	> 3753	215.3
(4_2^-)	5.387	5.287	3_1^-	4.352	4.945	M1	> 1.43	0.062
						E2	> 19.9	2.02
			4_1^-	4.831	4.902	M1	> 0.081	0.002
						E2	> 35.93	0.49
			5_1^-	4.942	5.167	M1	> 2.69	43.2
						E2	> 203.60	51.26
			(3_2^-)	4.949	5.464	M1	> 3.04	0.051
						E2	> 224	0.096
(6_2^+)	5.399	5.419	6_1^+	4.716	4.693	M1	> 7.16	0.94
						E2	> 224	72.0
(8_2^+)	5.478	5.571	8_1^+	4.848	4.910	M1	> 11.46	12.56
						E2	> 399	3.20
(7_2^+)	5.629	5.547	6_1^+	4.716	4.693	M1	$3.6(^{+16}_{-9})$	0.12
								(0.47)
						E2	$59(^{+28}_{-16})$	2.58
								(27.03)
			8_1^+	4.848	4.910	M1	$2.3(^{+11}_{-5})$	7.71
								(0.9907)
						E2	$56(^{+24}_{-12})$	20.40
								(1.40)
			7_1^+	4.919	4.934	M1	$1.2(^{+5}_{-4})$	6.37
								(6.65)
						E2	$36(^{+16}_{-8})$	0.28
								(14.61)
			(6_2^+)	5.399	5.419	M1	$10.7(^{+54}_{-36})$	46.8
								(80.74)
						E2	$3034(^{+1357}_{-758})$	11.80
								(72.56)
			(8_2^+)	5.478	5.571	M1	$16.1(^{+76}_{-36}) \times 10^{-2}$	325.2
								(92.34)
						E2	$8583(^{+3792}_{-2155})$	186.6
								(51.28)
(6_3^+)	5.753	5.867	6_1^+	4.716	4.693	M1	>1.27	0.951
						E2	>16	0.658
			(6_2^+)	5.399	5.419	M1	> 9.85	3.77
						E2	> 1118	0.375

Table 1. The comparison of theoretical transition rates of yrast and non-yrast states of ^{132}Sn with experimental data [11]. The B(M1) values are quoted in unit of $10^{-3} \times {\mu_n}^2$. The B(E2) values are in unit of $e^2 fm^4$. See text for values of effective operators. The details of parenthesis is given in text.

rates or an experimental limit have been evaluated using measured lifetimes and branching ratios derived from the $\beta-$decay of ^{132}In.

The yrast 5^+ state de-excites to 4_1^+ and 6_1^+ state by emitting γ-rays. For the transition from 5_1^+ to 4_1^+ state, the theoretical result aligns well with the experimental limit for the magnetic transition. However, it underestimates the E2 strength, even with a higher neutron effective charge e_n^{eff}. A similar observation is seen for transition to 6_1^+ state.

Using the same quenched $g^s_{\pi/\nu}$-factors and e_n^{eff}= 1.2e, we have also evaluated the transition probabilities of non-yrast states tabulated in table 1.

For the 4_2^- state, its decay to 3_1^- state is characterized by B(M1) > 0.00143 μ_n^2 and B(E2)> 19.9 e^2fm^4. But, our shell-model calculation underestimates these values. A possible explanation is the inability to reproduce the correct nature of 3_1^- state. It has collective nature and mainly results from superposition of different p-h configurations, already described in Ref. [19]. Additionally, 4_2^- is proposed in Ref. [11] to have a configuration of $\nu 3s_{1/2}^{-1}2f_{7/2}$. Whereas, the SM is predicting to have major contribution coming from $\nu 2d_{3/2}^{-1}1h_{9/2}$ (93%) for this state. Similar discrepancy is observed for $4_2^- \rightarrow 4_1^-$ transition. In our SM calculation, 4_1^- (E_{exp} = 4.831 MeV) state is predicted at 4.902 MeV with predominant configuration $\nu 2f_{7/2}2d_{3/2}^{-1}$ consistent with Ref. [11]. Although, for decay from 4_2^- to 5_1^- state, M1 transition rate agrees well with experimental estimate but discrepancy is observed for E2 rates. 5_1^- (E_{exp} = 4.942 MeV) state is evaluated at 5.167 MeV, with an 88% contribution coming from $\nu 1h_{9/2}2d_{3/2}^{-1}$ multiplet. But, according to Beinto *et al.* [11], this state is proposed to arise from $\nu 2f_{7/2}2d_{3/2}^{-1}$ multiplet, the same as 4_1^- state.

Another possible decay transition is reported from the 4_2^- state to an energy level at 4.949 MeV. This excited state is suggested to have angular momentum J = 3 with negative parity, based on the systematics of the transition, though no direct confirmation of the parity as well as angular momenta is available. Assuming this level corresponds to the second 3^- state, the shell-model predicts it at relatively higher energy (5.464 MeV). It has mixed contributions generated from the $\nu 2d_{3/2}^{-1}3p_{3/2}$(60%) and $\nu 3s_{1/2}^{-1}2f_{7/2}$ (37%) multiplets. The shell-model calculations underestimate both the magnetic and electric transition strengths for this decay as well.

In the 5-6 MeV energy range, a few new levels have been identified with the expected J = 4 to J = 8. Fogelberg *et al.* [24] identified the 5.399 MeV (6_2^+), 5.478 MeV (8_2^+), and 5.629 MeV (7_2^+) states as members of $\pi 1g_{9/2}^{-1}1g_{7/2}$ multiplet. In this energy range along with this proton configuration, neutron core exciting states such as $\nu 1h_{11/2}^{-1}2p_{3/2}$ or $\nu 3s_{1/2}^{-1}2f_{7/2}$ are also anticipated. As a result, possible configuration mixing hinders definitive assignments. Notably, our proton model space does not include the $\pi 1g_{9/2}$ orbital, which limits direct comparison with these states. In our calculation, second 6^+ state is evaluated at 5.419 MeV with dominant configuration of $\nu 1h_{11/2}^{-1}3p_{3/2}$ (94%). Whereas, 8_2^+ and 7_2^+ state are calculated at energy 5.571 and 5.547 MeV respectively, with predominant configuration of $\nu 1h_{11/2}^{-1}1h_{9/2}$ contributing 98% and 78% amplitudes respectively. Experimentally, the excited 7_2^+ state is observed to decay to various levels through M1+E2 transition. The calculated transition probabilities associated to 7_2^+ state underestimate the observed values. A slight improvement, particularly for E2 transition is observed when theoretical 7_3^+ state is considered as a parent state except for $8_{1,2}^+$ states. The corresponding transition strength is given in parenthesis in table 1. This 7_3^+ (E_{SM}=5.688 MeV) state has $\nu 1h_{11/2}^{-1}2p_{3/2}$ configuration, according to shell-model calculations.

Similar, observation is seen for transition strngth of 6_3^+ also. As per Ref. [11], this level is arising due to $\nu 1h_{11/2}^{-1}2p_{3/2}$ partition. But the calculated ones has $\nu 1h_{11/2}^{-1}1h_{9/2}$ configuration.

In the higher energy interval (6-7 MeV), the identification of states becomes increasingly challenging due to the numerous possible particle-hole (p-h) multiplets and the likely admixture of configurations. Consequently, our analysis has been limited to calculating the transition strengths of those associated levels.

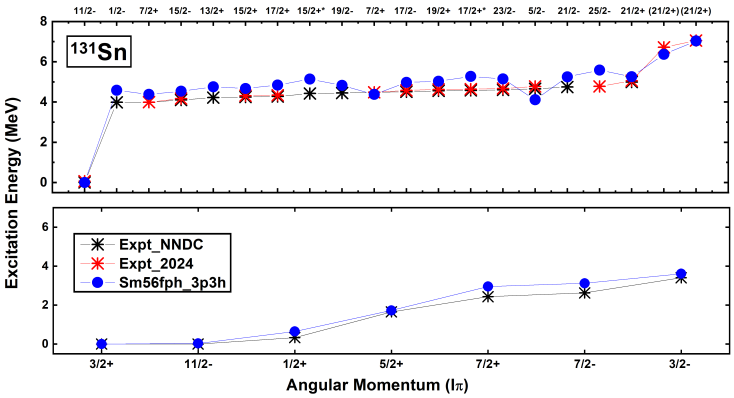

Figure 2. Comparison of experimental spectra of ^{131}Sn with theory. Recent data from Ref. [15] marked as Expt_2024 and data extracted from NNDC[5] as Expt_NNDC. More details are mentioned in the legend, caption of Fig.1.

3.2 Results on $^{131}_{50}Sn_{81}$

This particular nucleus has significance as it can be described as single neutron hole relative to $^{132}_{50}$Sn. The very recent experiment has clarified the ambiguity regarding to the position of first-excited $\nu 1h_{11/2}$ state through an independent mass spectroscopy experiment conducted at IGISOL facility [15]. This study expanded the level scheme by including 22 newly identified excited levels and 31 new γ-transitions. We have calculated the energy states using 3p3h mode where a maximum of three neutrons can be excited above the N=82 orbitals, each having one particle. The details of previously known levels are already discussed in Ref. [19]. We have compared our theoretical result with this newly available data and ENSDF data[5], as shown in Fig. 2. The excited levels at energy 6.720 MeV and 7.053 MeV are assigned as $(21/2^+)$ in Ref. [15]. As per our shell-model calculation, it corresponds to 3rd and 4th $21/2^+$ state. The $21/2^+_3$ state is mainly arising from the configuration $\nu 2d^{-1}_{3/2}1h^{-1}_{11/2}1h_{9/2}$ configuration. Whereas, $21/2^+_4$ state has mixed configuration of $\nu 3s^{-1}_{1/2}1h^{-1}_{11/2}1h_{9/2}$ (68%) and $\nu 2d^{-1}_{5/2}1h^{-1}_{11/2}1h_{9/2}$ (25%).

The decay transition from $(1/2^+_1) \rightarrow (3/2^+_1)$ is important as it carries direct information about the single particle states. Our calculation underestimated this value by a factor of 10^2 as tabulated in table 2. The underlying reason may be the non existence of $\pi 1g_{9/2}$ orbit lying below $Z = 50$ shell, in our model space. The enhancement of M1 transitions can be described by including the polarization effect of the core as suggested in Ref. [15].

The 4.513 MeV excited state with $J^\pi = (19/2)^-$ is identified as member of the $\nu 1h^{-2}_{11/2}2f_{7/2}$ configuration, consistent with our calculation showing a 96% contribution. Lifetime measurements of this state provide definitive information about the E4 transition to the $11/2^-_1$ state, for which only an upper limit was previously available. This level also de excites to $(15/2)^-_1$ and $(17/2)^+_1$ via E2 and E1 transition respectively. The $(15/2)^-_1$ state is has similar configuration as $(19/2)^-_1$ (98%). The calculated B(Eλ) values show better agreement with experimental results for multipolarity, λ= 2, 4 than for λ=1. The $(17/2)^+_1$ state is theoretically arising from $\nu 2d^{-1}_{3/2}1h^{-1}_{11/2}2f_{7/2}$ with 82% amplitude. In Benito *et al.,* this yrast state is described as $\nu 1h^{-2}_{11/2} \bigotimes 3^-_1(^{132}Sn)$ state. The larger discrepancy for the E1 transition is likely due to the inexact description of 3^-_1 state of ^{132}Sn, which affects this state also. In present model space, $\nu 2f_{5/2}$, $\nu 3p_{1/2}$, and $\nu 1i_{13/2}$ orbits are excluded. These orbits typically have minimal

impact on the energy eigenvalues or transition rate of for λ= 2, 4. However, this exclusion affects B(E1) predictions, which arise from minor contributions of higher-shell orbits in the wave functions. Even small overlaps in wave functions are crucial for accurately reproducing experimental B(E1) values.

The calculated B(E2: $(23/2^-_1) \rightarrow (19/2^-_1)$) value shows reasonable agreement with the experimental data. Both states originate from the same multiplet as proposed in Ref. [15].

Both the $(23/2^-_1)$ and $(25/2^-_1)$ states are theoretically assigned the configuration $\nu 1h^{-2}_{11/2}2f_{7/2}$. However, $(25/2^-_1)$ state is suggested to originate from proton core excitation with a configuration $\pi 1g_{7/2}1g^{-1}_{9/2}\nu 1h^{-1}_{11/2}$ configuration. The calculated reduced magnetic transition strength for $(25/2^-_1) \rightarrow (23/2)^-_1$ is found to overestimate the experiment values.

J^π_i	$E_i(MeV)$		J^π_f	$E_f(MeV)$		Xλ	B(Xλ)	
	Expt.	Theo.		Expt.	Theo.		Expt.	Theo.
$(1/2^+)_1$	0.332	0.649	$3/2^+_1$	0.0	0.0	M1	$5.9(12) \times 10^{-2}$	0.086×10^{-2}
$(19/2^-)_1$	4.513	4.869	$11/2^-_1$	0.065	0.036	E4	$4.92(8) \times 10^5$	1.03×10^5
			$(15/2^-)_1$	4.168	4.572	E2	23.3(8)	8.64
			$(17/2^+)_1$	4.339	4.877	E1	$1.03(9) \times 10^{-4}$	4.00×10^{-7}
$(23/2^-)_1$	4.671	5.185	$(19/2)^-_1$	4.513	4.861	E2	13.43(11)	9.13
$(25/2^-)_1$	4.775	5.620	$(23/2^-)_1$	4.671	5.815	M1	$8.4(215) \times 10^{-4}$	3.11×10^{-2}
$(19/2^+)_1$	4.624	5.068	$(17/2^+)_1$	4.339	4.877	M1	$2.85(21) \times 10^{-2}$	19×10^{-2}

Table 2. The comparison of theoretical transition rates of yrast states of ^{131}Sn with experimental data [15]. The B(M1) values are quoted in unit of $\mu_n{}^2$. The B(Eλ) values are quoted in unit of $e^2 fm^{2\lambda}$. For E1 transition rate, e_p=1.64e and e_p=0.35e.

3.3 Interpretation

As noted in Ref.[19], cross-shell $\nu 1h^{-1}_{11/2}$ - $\nu 2f_{7/2}$ *tbme* values for the effective interaction were primarily tuned using the yrast states J^π= 2^+ to 9^+ excluding 3^+. However, the corresponding matrix elements for $\nu 1h^{-1}_{11/2} - \nu 3p_{3/2}$ could not be systematically refined due to limited experimental data. Only relevant *tbme* parameters were adjusted to improve predictions for 6^+_2 and 7^+_2 state. Similarly, two tbme for $\nu 1h^{-1}_{11/2}$-$\nu 1h_{9/2}$ coupling were tuned for better agreement with these states. The remaining *tbme* parameters remain untuned due to insufficient data. Based on recent experimental findings and empirical calculations, tentative assignments have been made for these new states[11, 15]. However, at higher energy ranges, multiple configurations and potential configuration mixing make it challenging to ascertain their exact nature. Refinement of matrix elements requires more comprehensive experimental data. Also, the mismatch of the values with experimental values can largely be attributed to the limitations of the restricted model space.

4 Conclusion

The excited states of ^{131,132}Sn have been investigated within the framework of shell-model calculations using a newly formulated cross-shell interaction. While some transitions show good agreement with experimental data, discrepancies are observed for others. The findings suggest that further fine-tuning of various cross-shell neutron-neutron *tbme*s is needed to improve theoretical prediction. Achieving this requires more refined knowledge of these excited states. Also, in some cases, it points to the necessity of expanding the model space by including proton orbitals below Z = 50.

5 Acknowledgement

The authors acknowledge the support from Prof. M. Saha Sarkar, Saha Institute of Nuclear Physics, Kolkata in developing the interaction. The authors further expresses gratitude to SERB-DST for providing the computational facility under Government of India Project No. EMR/2016/006339.

References

[1] M. Chartier *et al.*, Phys. Rev. Lett. **77**, 2400 (1996).
[2] C. B. Hinke *et al.*, Nature (London) **486**, 341 (2012).
[3] B. Fogelberg *et al.*, Phys.Rev. Lett. **73**, 2413 (1994).
[4] B. Fogelberg *et al.*, Phys. Scr. T56, **79** (1995).
[5] https://www.nndc.bnl.gov/
[6] K. L. Jones *et al.*, Nature (London) **465**, 454 (2010).
[7] V. Vaquero *et al.*, Phys. Rev. Lett. **118**, 202502 (2017).
[8] M. Górska *et al.*, Phys. Lett. B **672**, 313 (2009).
[9] J. Taprogge *et al.*, Phys. Rev. Lett. **112**, 132501 (2014).
[10] D. Rosiak *et al.*, Phys. Rev. Lett. **121**, 252501 (2018).
[11] J. Benito *et al.*, Phys. Rev. C **102**, 014328 (2020).
[12] K. Whitmore *et al.*, Phys. Rev. C **102**, 024327 (2020).
[13] J. Terasaki et al.,, Phys. Rev. C *66*, 054313 (2002).
[14] A. Ansari et al.,, Phys. Rev. C *74*, 054313 (2006).
[15] J. Benito *et al.*, Phys. Rev. C **110**, 014328 (2024).
[16] S. Bottoni *et al.*, Acta Phys. Pol. B **50**, 285 (2019).
[17] R. Dunlop *et al.*, Phys. Rev. C **99**, 045805 (2019).
[18] S. Mukhopadhyay *et al.*, **1000**, 121785 (2020).
[19] S. Das *et al.*, Nucl. Phys. A **1014**, 122262 (2020).
[20] B. A. Brown *et al.*, Phys. Rev. C **71**, 044317 (2005).
[21] B. A. Brown, W. D. M. Rae, Nucl. Data sheets **120**, 115 (2014).
[22] B. A. Brown, MSU-NSCL report number **1289** (2004).
[23] P. Bhattacharyya *et al.*, Phys. Rev. Lett. **87**, 062502 (2001).
[24] B. Fogelberg *et al.*, Phys. Rev. Lett. **73**, 2413 (1994)